UC San Diego
UC San Diego Previously Published Works

Title

Pelvic Blood Flow Predicts Fibroid Volume and Embolic Required for Uterine Fibroid Embolization: A Pilot Study With 4D Flow MR Angiography.

Permalink

https://escholarship.org/uc/item/9x40q46n

Journal

American Journal of Roentgenology, 210(1)

ISSN

0361-803X

Authors

Malone, Christopher D
Banerjee, Arjun
Alley, Marcus T
et al.

Publication Date

2018

DOI

10.2214/ajr.17.18127

Peer reviewed

Pelvic Blood Flow Predicts Fibroid Volume and Embolic Required for Uterine Fibroid Embolization: A Pilot Study With 4D Flow MR Angiography

Christopher D. Malone[1]
Arjun Banerjee[2]
Marcus T. Alley[3]
Shreyas S. Vasanawala[3]
Anne C. Roberts[1]
Albert Hsiao[1]

[1]Department of Radiology, University of California, San Diego, 200 W Arbor Dr, MC 0834, San Diego, CA 92103-0834. Address correspondence to C. D. Malone (cmalone05@gmail.com).

[2]School of Medicine, University of California, San Diego, La Jolla, CA.

[3]Department of Radiology, Stanford University School of Medicine, Stanford, CA.

OBJECTIVE. We report here an initial experience using 4D flow MRI in pelvic imaging—specifically, in imaging uterine fibroids. We hypothesized that blood flow might correlate with fibroid volume and that quantifying blood flow might help to predict the amount of embolic required to achieve stasis at subsequent uterine fibroid embolization (UFE).

MATERIALS AND METHODS. Thirty-three patients with uterine fibroids and seven control subjects underwent pelvic MRI with 4D flow imaging. Of the patients with fibroids, 10 underwent 4D flow imaging before UFE and seven after UFE; in the remaining 16 patients with fibroids, UFE had yet to be performed. Four-dimensional flow measurements were performed using Arterys CV Flow. The flow fraction of the internal iliac artery was expressed as the ratio of internal iliac artery flow to external iliac artery flow and was compared between groups. The flow ratios between the internal iliac arteries on each side were calculated. Fibroid volume versus internal iliac flow fraction, embolic volume versus internal iliac flow fraction, and embolic volume ratio between sides versus the ratio of internal iliac artery flows between sides were compared.

RESULTS. The mean internal iliac flow fraction was significantly higher in the 26 patients who underwent imaging before UFE (mean ± standard error, 0.78 ± 0.06) than in the seven patients who underwent imaging after UFE (0.48 ± 0.07, $p < 0.01$) and in the seven control patients without fibroids (0.48 ± 0.08, $p < 0.0001$). The internal iliac flow fraction correlated well with fibroid volumes before UFE ($r = 0.7754$, $p < 0.0001$) and did not correlate with fibroid volumes after UFE ($r = -0.3051$, $p = 0.51$). The ratio of embolic required to achieve stasis between sides showed a modest correlation with the ratio of internal iliac flow ($r = 0.6776$, $p = 0.03$).

CONCLUSION. Internal iliac flow measured by 4D flow MRI correlates with fibroid volume and is predictive of the ratio of embolic required to achieve stasis on each side at subsequent UFE and may be useful for preprocedural evaluation of patients with uterine fibroids.

Accurate and noninvasive assessment of pelvic blood flow is a potentially valuable clinical tool for evaluating patients with pelvic abnormalities, including uterine fibroids. Ultrasound (US) is often used as the first-line imaging modality to identify fibroids but can be limited by operator experience and sonographic windows and does not allow quantification of blood flow. MRI is often performed for routine evaluation before uterine fibroid embolization (UFE) because of its ability to more fully depict and characterize fibroids, provide soft-tissue characterization including degree of degeneration and necrosis [1], and delineate the anatomy of the uterus and adjacent pelvic structures [2]. Recent improvements and availability of 4D flow MRI are now on the cusp of making routine quantification of blood flow clinically feasible and robust [3–5].

These characteristics of MRI may provide interventionalists and gynecologists with more comprehensive information to guide the optimal management of patients.

UFE has emerged as a mainstay treatment of uterine fibroids because of its efficacy and its minimally invasive nature [6, 7]. UFE relies on delivery of embolic particles through the vasculature supplying the fibroids, usually facilitated by high flow in the uterine artery, resulting in fibroid ischemia, necrosis, and volume reduction [8–11]. Although UFE is an attractive method for treatment, several characteristics are considered when selecting patients who would benefit from this therapy. Uterine fibroids characterized as hypervascular have longer regrowth-free intervals after UFE than their hypovascular counterparts [12, 13]. In addition, the degree of UFE-induced necrosis has been shown to

correlate with improved clinical outcomes [14, 15]. It is therefore possible that measurement of arterial blood flow may be complementary to other MRI techniques in the evaluation of patients before and after UFE.

The current MRI techniques for evaluating fibroid vascularity include quantifying enhancement with time–signal intensity curves and evaluating perfusion [9, 16–19]. However, these methods do not measure actual blood flow; instead, they show extracellular leakage of gadolinium contrast agents into the highly leaky interstitial space of a fibroid [17]. Although not routinely performed at all centers, MR angiography (MRA) can provide additional information regarding fibroid vasculature including uterine artery anatomy and extrauterine blood supply sources such as the ovarian artery or other vessels [20–25]. Traditional MRA can provide exquisite detail of vascular anatomy and a road map before UFE, but it does not quantify blood flow unless phase-contrast techniques are used.

Over the past decade, time-resolved 3D phase-contrast MRA (4D flow imaging) has emerged as a robust tool to assess flow in the cardiovascular system, especially in the context of congenital heart disease and aortic aneurysms by acquiring phase-contrast velocity data in 3D [26–28]. Its use has also been expanded to include the abdomen for assessment of portal hepatic flow [3, 29, 30]. Four-dimensional flow imaging allows quantification of blood flow in any plane after acquisition, which is a significant advancement from the conventional 2D phase-contrast MRI approach that is more often used. The latter requires precise planes to be prescribed before each acquisition, requiring significant operator expertise and a priori knowledge of the vessel of interest [4]. In recent years, acquisition of 4D flow data has become more efficient through accelerated scanning techniques such as compressed-sensing and parallel imaging [5, 31]. These techniques have significantly shortened 4D flow scanning time to enable its incorporation into routine MRI protocols, whereas before the time needed for scanning was prohibitive.

At the University of California, San Diego, we have added a highly accelerated variant of 4D flow MRI to our routine pelvic MRI protocol for patients being clinically assessed for uterine fibroids. In this pilot study, we aimed to assess the potential value of 4D flow imaging for the assessment of pelvic arterial flow before UFE. We hypothesized that measurements of blood flow from

4D flow imaging might be able to provide additional information previously inaccessible by MRI. We compared blood flow in patients with fibroids and control subjects without fibroids. We also compared blood flow in patients with fibroids with fibroid volume and laterality and the amount of embolic required at subsequent UFE. Finally, we postulated that lower blood flow as assessed by 4D flow imaging would be detected in patients who had undergone UFE with a subsequent decrease in the size of their fibroids.

Materials and Methods

We obtained institutional review board approval at the University of California San Diego to retrospectively review the records of patients who underwent routine pelvic MRI including 4D flow imaging between September 2015 and November 2016 in a manner compliant with HIPAA. This review included MRI examinations of 33 patients with uterine fibroids and seven control patients who underwent pelvic MRI for other issues not related to fibroids or other uterine abnormalities. Of the patients with fibroids, 10 underwent 4D flow imaging before UFE and seven after UFE; the remaining 16 patients with fibroids had yet to undergo UFE.

For patients who underwent UFE after MRI with 4D flow imaging, the total volume of nonspherical polyvinyl alcohol (PVA) particles (PVA Foam Embolization Particles, Cook Medical) required for uterine artery stasis was tabulated from procedure reports. In brief, the UFE procedure was initiated with right common femoral arterial access followed by an aortogram obtained using a catheter (Omni Flush, AngioDynamics) at the level of the renal arteries with imaging centered at the pelvic region. The Omni Flush catheter was exchanged for either a uterine catheter (Roberts Uterine Catheter, Cook Medical) or a long reverse curve uterine catheter (Impress, Merit Medical Systems), with subsequent selection and angiograms at the origins of both uterine arteries. A coaxial microcatheter (Maestro, Merit Medical Systems) was used only if the uterine artery was small or if its origin was sharply angled.

At our institution, embolization was initiated with 200-μm PVA particles, which ranged between 180 and 300 μm in diameter, followed by 300-μm PVA particles, which ranged between 300 and 500 μm in diameter. The volume of embolic delivered refers to the original dry volume of embolic before reconstitution in 20 mL of iohexol 240 (Omnipaque 240, GE Healthcare), and the volume of embolic was tabulated during the procedure by the interventional radiology technologist. Each vial of PVA particles consisted of 1 mL of total dry embolic. Embolization of each uterine artery was per-

formed until stasis within the artery was achieved. Final completion angiograms with hand injection on each side were obtained to confirm nonfilling of the uterine artery. The interventional radiologist performing UFE was not aware of the flow measurements before or during the procedure.

All MRI examinations were performed on the same 3-T MRI unit (GE Discovery MR750 3T, GE Healthcare) using a 32-channel body-array coil. Conventional protocol sequences included coronal and axial T2-weighted single-shot fast spin-echo (FSE), sagittal and oblique axial T2-weighted fast-relaxation FSE, and axial DWI (b value = 500–1000 s/mm^2). Multiphasic dynamic contrast-enhanced MRI (gadobutrol [Gadavist 0.1 mL/kg, Bayer HealthCare Pharmaceuticals]) was performed using differential subsampling with Cartesian ordering (DISCO) [32]. This sequence was followed by a contrast-enhanced liver acquisition with volume acceleration (LAVA-Flex, GE Healthcare) sequence in the axial, sagittal, and coronal planes. Contrast-enhanced 4D flow MRI was then performed using a retrospectively cardiac-gated spoiled gradient-recalled sequence with 4-point encoding, a 15° flip angle, TR/TE of 5.5/2.9, and bandwidth of 62 kHz. The typical acquired spatial resolution was 2.1 × 2.8 × 1.6 mm (right-left × anterior-posterior × inferior-superior) and the velocity-encoding speed was 120 cm/s. This sequence was optimized using combined parallel imaging, compressed sensing, and respiratory self-navigation for a total acceleration of 6.4 (3.2 phase × 2.0 slice) [31, 33]. The average scanning time for the 4D flow sequence was 8–12 minutes, and scanning was performed during free breathing.

Up to four uterine fibroids were measured in three orthogonal dimensions on conventional T2-weighted or contrast-enhanced LAVA-Flex sequences in each patient. Clusters of more than three fibroids were measured in conglomerate. Fibroid volumes were summed for each patient, and reviewers noted if fibroids exhibited a lack of enhancement or exhibited necrosis.

In the 26 patients who had not undergone UFE, the volume of necrosis was subtracted from the total fibroid volume. Patients showing twice the fibroid volume or greater on one side of the endometrium versus the other were considered to have anatomic laterality of their fibroids.

All 4D flow measurements were made using Arterys CV Flow (Arterys). Flow was measured (in liters per minute) with orthogonal ROIs at the distal aorta just before the iliac bifurcation, bilateral common iliac arteries, external iliac arteries, and proximal internal iliac arteries in triplicate locations for each vessel (Fig. 1). Ovarian artery flow was measured when the blood supply to the fibroids was detected on DISCO images. The total

TABLE 1: Demographic and Procedure Characteristics and Mean Flow Values of Patient Groups

Characteristic	Patients With Fibroids		Control Subjects (n = 7)
	Before UFE (n = 26)	After UFE (n = 7)	
Age at MRI (y)	44.1 ± 10.6	43.0 ± 9.4	47.6 ± 9.0
Weight (kg)	68.8 ± 14.3	65.6 ± 10.2	66.5 ± 11.5
Body mass index[a]	25.6 ± 5.5	24.2 ± 4.0	25.7 ± 6.3
Fibroid volume (mL)	4030.1 ± 2427.8	1299.7 ± 1101.0	NA
Time from MRI to UFE, if applicable (mo)	2.0 ± 0.9	NA	NA
Time from UFE to MRI, if applicable (mo)	NA	47.1 ± 37.8	NA
No. of UFEs	[b]	1.1 ± 0.4	NA
Flow (L/min)			
Distal aorta	1.33 ± 0.30	1.07 ± 0.40	1.49 ± 0.47
Right common iliac artery	0.66 ± 0.16	0.52 ± 0.18	0.77 ± 0.27
Right external iliac artery	0.38 ± 0.11	0.35 ± 0.16	0.57 ± 0.26
Right internal iliac artery	0.28 ± 0.10	0.17 ± 0.03	0.26 ± 0.10
Left common iliac artery	0.60 ± 0.18	0.50 ± 0.19	0.71 ± 0.24
Left external iliac artery	0.36 ± 0.12	0.37 ± 0.18	0.53 ± 0.23
Left internal iliac artery	0.25 ± 0.09	0.13 ± 0.04	0.25 ± 0.12

Note—Data are presented as mean ± standard error. UFE = uterine fibroid embolization, NA = not applicable.
[a]Weight in kilograms divided by the square of height in meters.
[b]All patients had one UFE session when it was performed after 4D flow imaging.

internal iliac flow fraction was measured as the ratio of the internal iliac artery flow to external iliac artery flow for each patient. Flow fractions were used to address potential variations in flow between patients due to other factors such as body mass or underlying atherosclerotic disease. Separate internal iliac flow fractions were also calculated for each contralateral side. Contralateral flow differences were measured by comparing flow ratios between internal iliac arteries on each side.

To assess internal consistency in flow measurements, we constructed Bland-Altman plots comparing summed flow in the bilateral common iliac arteries with that of the distal aorta and comparing summed flows of both the internal and external iliac arteries with the common iliac arteries. Patient characteristics, demographics, and average flow measurements among groups are shown in Table 1.

Total internal iliac flow fractions were compared between control subjects, patients with fibroids who underwent imaging before UFE, and patients with fibroids who underwent imaging after UFE. Contralateral internal iliac flow differences were compared between control subjects and patients with and without fibroid anatomic laterality. In patients who underwent MRI before UFE, differences between contralateral internal iliac flow values and internal iliac flow ratios were correlated with the ratio of embolic volume required to stasis between each side. Statistical sig-

nificance between all groups was determined using unpaired two-tailed t tests with a type 1 error rate (α) of 0.05. Fibroid volume versus total internal iliac flow fractions, total volume of PVA embolic versus internal iliac flow fraction for each side, and the ratio of embolic volume between sides versus the ratio of internal iliac artery flows between sides were plotted, and Pearson correlation coefficients were calculated. Data are presented as mean ± standard error (SE).

Results

Internal Iliac Flow Fractions in Patients With Fibroids and Control Subjects

We assessed pelvic arterial blood flow with 4D flow imaging by quantifying the internal iliac flow fraction as the ratio of internal iliac arterial flow to external iliac arterial flow. Elevated internal iliac artery flow was seen in the 26 patients with fibroids who underwent imaging before UFE; imaging showed that the total internal iliac artery flow was actually greater than that of the external iliac artery flow in six of these 26 patients and that at least one side showed higher internal iliac arterial flow than external iliac arterial flow in eight of the 26 patients (Fig. 2). The mean internal iliac flow fraction in the 26 patients with fibroids who underwent imaging before UFE was significant-

ly higher (mean ± SE, 0.78 ± 0.06), reflecting underlying fibroid hypervascularity, than that in the seven patients with fibroids who underwent imaging after UFE (0.48 ± 0.07, $p < 0.01$) and the seven control subjects without fibroids (0.48 ± 0.08, $p < 0.0001$) (Fig. 3). These differences were readily apparent on oblique vector-overlay 4D flow views profiling the external and internal iliac arteries side-by-side. More robust flow in the internal iliac artery of pre-UFE fibroid patients was clearly seen compared with post-UFE fibroid patients and control subjects (Fig. 4). Internal iliac flow fractions correlated well with fibroid volumes in patients with fibroids who underwent imaging before UFE ($r = 0.7754$, $p < 0.0001$) (Fig. 5). However, we did not see this correlation in patients with fibroids who underwent imaging after UFE ($r = -0.3051$, $p = 0.51$), likely reflecting underlying devascularization with necrosis occurring to a greater extent than fibroid volume reduction.

Laterality of Internal Iliac Flow Detected by 4D Flow Imaging

We assessed pelvic flow laterality by comparing the ratio of internal iliac artery flows between sides in each patient and compared with fibroid anatomic laterality. Anatomic laterality matched flow laterality in 12 of 15 patients but showed a wide distribution of flow ratios between internal iliac arteries on each side that were not significantly different from those of patients without anatomic laterality (Fig. 6). This observation was likely contributed to supply from the contralateral vasculature. Mean flow ratios between internal iliac arteries on each side for fibroid patients with and those without anatomic laterality were 1.54 ± 0.14 ($n = 12$ patients) and 1.42 ± 0.10 ($n = 18$ patients) ($p = 0.39$), respectively. Control patients without fibroids had a mean flow ratio between the internal iliac arteries on each side of 1.12 ± 0.03, which was significantly lower than the values in fibroid patients with and those without anatomic laterality (both, $p < 0.01$).

In keeping with the wide distribution of flow ratios between internal iliac arteries on each side in fibroid patients, 4D flow imaging may highlight differences in flow that are not readily apparent on conventional MRA or catheter angiography. Figures 7A and 7B show a patient with a single midline fibroid (patient 7 in Table 2), with apparent equal contributions from both uterine arteries seen on DISCO MRA. Four-dimensional flow imaging (Figs. 7C and 7D) performed

TABLE 2: 4D Flow Imaging and Uterine Fibroid Embolization (UFE) Procedural Data for Patients Who Underwent MRI With 4D Flow Imaging Before UFE

Patient No.	Total Fibroid Volume (mL)	Right Internal Iliac Artery		Left Internal Iliac Artery		Contralateral Internal Iliac Flow Ratio	Embolic Volumes[a] (mL)		Embolic Volume Ratio Between Sides
		Flow Fraction	Flow (L/min)	Flow Fraction	Flow (L/min)		Right Side	Left Side	
1	680.6	**0.84**	**0.27**	0.55	0.10	2.76	**0.75 (300 μm); 0.85 (200 μm)**	0 (300 μm); 0.15 (200 μm)	10.67
2	2736.7	0.51	0.22	**0.74**	**0.30**	1.38	1.5 (300 μm); 0.5 (200 μm)	**2.5 (300 μm); 0.5 (200 μm)**	1.50
3	5508.6	**1.42**	**0.39**	1.09	0.29	1.36	**1.5 (300 μm); 0.5 (200 μm)**	1.0 (300 μm); 0.5 (200 μm)	1.33
4[b]	6541.5	**0.87**	**0.24**	0.51	0.12	1.92	**5.0 (300 μm); 0.7 (200 μm)**	0 (300 μm); 0.3 (200 μm)	19.00
5	9829.1	0.91	0.21	**1.92**	**0.31**	1.49	1.25 (300 μm); 0.5 (200 μm)	**1.75 (300 μm); 0.5 (200 μm)**	2.75
6	2981.4	**0.82**	**0.38**	0.61	0.29	1.31	1.25 (300 μm); 0.5 (200 μm)	**1.75 (300 μm); 0.5 (200 μm)**	1.29
7	3509.5	**0.58**	**0.26**	0.51	0.17	1.54	**3.0 (300 μm); 0.5 (200 μm)**	1.0 (300 μm); 0.5 (200 μm)	2.33
8	4749.4	0.64	0.38	**0.70**	**0.39**	1.02	1.75 (300 μm); 0.5 (200 μm)	**2.0 (300 μm); 0.5 (200 μm)**	1.11
9	1087.5	0.27	0.14	**0.37**	**0.18**	1.31	0.25 (300 μm); 0.5 (200 μm)	**1.0 (300 μm); 0.5 (200 μm)**	2.00
10	4663.9	0.81	0.23	**0.89**	**0.25**	1.10	0.25 (300 μm); 0.5 (200 μm)	**2.0 (300 μm); 0.5 (200 μm)**	3.33

Note—Boldface values indicate the side that showed higher flow and that required greater volume of embolic to achieve stasis.

[a]Values in parentheses are diameters of polyvinyl alcohol particles.

[b]Left ovarian artery supply to fibroids. Flow was 0.04 L/min. Fibroids were subsequently embolized with 0.75 mL of 200-μm polyvinyl alcohol particles.

before UFE showed higher flow in the right internal iliac artery than in the left (0.26 vs 0.17 L/min). A pelvic aortogram obtained at subsequent UFE showed roughly equal conspicuity of both uterine arteries, with each supplying a large proportion of the fibroid on subsequent selective injections (Figs. 7E–7G). The right side required more than twice the volume of embolic to achieve stasis (0.5 mL of 200-μm PVA particles and 3.0 mL of 300-μm PVA particles) compared with the left (0.5 mL of 200-μm PVA particles and 1.0 mL of 300-μm PVA particles).

4D Flow Imaging and Uterine Fibroid Embolization

We aimed to assess whether 4D flow imaging could predict embolic requirements at UFE by comparing gross flow (in liters per minute) and unilateral internal iliac flow fraction with the required volume of embolic to stasis. We saw positive correlations between volume of PVA embolic required to stasis on each side with both unilateral internal iliac flow fractions ($r = 0.5423$, $p = 0.10$ [Fig. 8A]) and gross flow ($r = 0.4156$, $p = 0.23$ [Fig. 8B]). The greatest differences in volume required to stasis between different

patients were seen with the larger 300-μm PVA particles. When looking at differences in flow and embolic used between contralateral sides, a stronger positive correlation was seen between the ratio of PVA embolic required to stasis between sides and the contralateral internal iliac flow ratio ($r = 0.6776$, $p = 0.03$ [Fig. 8C]). Differences in flow between contralateral internal iliac arteries identified by 4D flow imaging correctly predicted which side would require a higher volume of PVA embolic to stasis in nine of 10 patients who later underwent UFE (Table 2). In the one patient with a mismatch between the side requiring a higher volume of embolic and the side with higher flow, the differences between both respective values were minimal (patient 6 in Table 2).

Contribution of Ovarian Artery Flow as Assessed by 4D Flow Imaging

We detected that the ovarian artery was contributing to fibroid vascular supply on the multiphasic DISCO sequence in two patients, one of whom later underwent UFE (patient 4 in Table 2). In this latter patient, the left ovarian artery was supplying the left side of her single right-sided fibroid, with 0.04 L/min of

flow as assessed by 4D flow imaging (Figs. 9A–9C). The second patient had a more substantial ovarian artery contribution, with bilateral supply to her fibroids (Figs. 9D–9G).

Internal Consistency of Flow Measurements

To confirm consistency and accuracy of flow measurements by 4D flow imaging, we compared the sum of flow measurements of downstream vessels—that is, the flow of the distal abdominal aorta with the sum of flow of the bilateral common iliac arteries and both common iliac arteries with the sum of their respective downstream external and internal iliac arteries. Bland-Altman plots were constructed for each comparison, as shown in Figure 10. Almost all measurements fell within 2 SDs of the flow differences between the vessel of interest and its downstream counterparts, indicating internal consistency of measurements.

Discussion

In this study, we show the clinical feasibility of 4D flow MRI for quantifying blood flow in the pelvis. To our knowledge, this study is the first application of this technique to this clinical indication, and our results illustrate its broader potential for pelvic imaging. We

observed that internal iliac flow not only correlated with fibroid volume but also predicted the amount of embolic required for stasis on each side at subsequent embolization. Before embolization, patients with uterine fibroids had significantly higher internal iliac flow fractions (internal iliac flow fraction ratios) than control patients without fibroids. This difference reflects the typical hypervascular nature of fibroids [12]. After UFE, internal iliac flow fractions significantly decreased. Because the goal of UFE is to devascularize the fibroids, rendering them ischemic, this result is not surprising; internal iliac flow fraction values were substantially lower in post-UFE patients who had subsequent decrease in fibroid size, suggesting that internal iliac flow fraction may be a useful metric to incorporate into the postprocedural evaluation of UFE patients. In addition, although it is difficult to predict blood flow asymmetry from anatomic imaging alone, measurement of internal iliac blood flow appears to better predict the amount of embolic required. This not only may provide value for procedural planning but also shows its potential as a clinical tool in studying the occasionally complex underlying vascular supply to uterine fibroids.

We were able to show that 4D flow imaging could reliably predict the side and amount of embolic required for stasis at subsequent UFE. Although it may be difficult to directly correlate flow values to discrete volumes of embolic, this observation can serve as a semiquantitative validation measure, because it is presumed that higher flows will require more volume to achieve stasis and vice versa. Most accepted UFE protocols call for evaluating and embolizing both uterine arteries, but differentiation of flow laterality may be of value for practitioners who have advocated a unilateral approach in the appropriate clinical setting [34]. Regardless, knowledge of potentially requiring higher embolic volumes on a particular side based on 4D flow data, especially when the differences are not apparent on conventional MRI or even catheter angiography, may help anticipate procedural requirements and potentially increase efficiency. The exact volumes required to stasis may differ with other types of embolic agents depending on their physical properties. However, our results with nonspherical PVA particles suggest that flow values would potentially correspond to embolic volumes among cohorts of patients who undergo embolization with different agents. However, this theory needs to be validated with additional studies.

Ovarian artery supply to fibroids can occur in up to 10% of patients and can be a frequent cause of treatment failure when only the uterine arteries are embolized [35, 36]. Knowledge of not only the presence of ovarian artery supply, but also quantification of its flow to fibroids can serve as valuable information regarding the significance of its contribution. Although ovarian artery supply was identified in only two of our patients using a high spatiotemporal resolution anatomic DISCO sequence in our protocol, we were able to show that 4D flow imaging could reliably delineate and quantify the flow in these vessels. These results further suggest an additional application for 4D flow imaging in evaluating patients with fibroids before and after UFE.

Our results suggest that 4D flow imaging may have an application in evaluating patients before and after UFE. Although the interventional radiologists performing the procedures were not aware of the 4D flow imaging results before, during, or after embolization, the results of this study suggest that 4D flow imaging may add valuable information moving forward and also opens doors for future studies. Four-dimensional flow imaging may highlight fibroid patients with lower-than-expected internal iliac artery flows, which may indicate that those fibroids are less dependent on blood flow and may not respond as well to UFE. In addition, 4D flow imaging after UFE may show the efficacy of embolization by measuring the extent of flow decrease, which could be incorporated with other postprocedural indicators of treatment success, such as fibroid size and enhancement and decrease in symptoms. Both of these issues are subject to future work.

Our study has several limitations. This is a single-center retrospective study of a relatively small number of patients, and as a pilot study, does not have longitudinal flow measurements before and after UFE for the same patients. Future studies may be helpful to compare whether internal iliac flow fraction may better predict resolution of fibroid symptoms than residual post-UFE fibroid volume. In addition, blood flow was assessed in the proximal internal iliac artery rather than the uterine artery, because of the small size of the uterine arteries and nonvisualization of the uterine arteries in control subjects. Regarding UFE, there is some natural subjectivity of the performing interventionalists on the size and volume of embolic used to achieve stasis. Finally, although we did not correlate our flow measurements with a

confirmatory modality, extensive prior work has shown that 4D flow imaging has excellent agreement with well-established methods of measuring flow such as catheter angiography, ultrasound, and 2D phase-contrast MRI [37–40]. Further validation and work to optimize the accuracy and precision of flow measurements in small arteries such as the uterine and ovarian arteries are expected in the future. As the 4D flow imaging technique continues to advance and evolve, longitudinal measurements in the same patients before and after UFE will provide additional insights into flow as a biomarker and predictor of treatment response. As of 2017, 4D flow MRI is available at only select academic institutions and is predominantly applied to the evaluation of thoracic cardiovascular system and portal venous system. However, as more MRI vendors implement this technique, we expect its use and availability to expand and may find that it is useful in the assessment of other pelvic vascular pathologic entities such as pelvic congestion.

References

1. Nieuwenhuis LL, Betjes HE, Hehenkamp WJ, Heymans MW, Brolmann HA, Huirne JA. The use of 3D power Doppler ultrasound in the quantification of blood vessels in uterine fibroids: feasibility and reproducibility. *J Clin Ultrasound* 2015; 43:171–178

2. Ghai S, Rajan DK, Benjamin MS, Asch MR, Ghai S. Uterine artery embolization for leiomyomas: pre- and postprocedural evaluation with US. *RadioGraphics* 2005; 25:1159–1172; discussion, 1173–1176

3. Roldan-Alzate A, Francois CJ, Wieben O, Reeder SB. Emerging applications of abdominal 4D flow MRI. *AJR* 2016; 207:58–66

4. Chelu RG, Wanambiro KW, Hsiao A, et al. Cloud-processed 4D CMR flow imaging for pulmonary flow quantification. *Eur J Radiol* 2016; 85:1849–1856

5. Tariq U, Hsiao A, Alley M, Zhang T, Lustig M, Vasanawala SS. Venous and arterial flow quantification are equally accurate and precise with parallel imaging compressed sensing 4D phase contrast MRI. *J Magn Reson Imaging* 2013; 37:1419–1426

6. de Bruijn AM, Ankum WM, Reekers JA, et al. Uterine artery embolization vs hysterectomy in the treatment of symptomatic uterine fibroids: 10-year outcomes from the randomized EMMY trial. *Am J Obstet Gynecol* 2016; 21:745.e1–745.e12

7. Spies JB, Cornell C, Worthington-Kirsch R, Lipman JC, Benenati JF. Long-term outcome from uterine fibroid embolization with tris-acryl gelatin microspheres: results of a multicenter study. *J Vasc Interv Radiol* 2007; 18:203–207

8. deSouza NM, Williams AD. Uterine arterial embolization for leiomyomas: perfusion and volume

changes at MR imaging and relation to clinical outcome. *Radiology* 2002; 222:367–374

9. Chapiro J, Duran R, Lin M, et al. Three-dimensional quantitative assessment of uterine fibroid response after uterine artery embolization using contrast-enhanced MR imaging. *J Vasc Interv Radiol* 2015; 26:670–678

10. Scheurig-Muenkler C, Wagner M, Franiel T, Hamm B, Kroencke TJ. Effect of uterine artery embolization on uterine and leiomyoma perfusion: evidence of transient myometrial ischemia on magnetic resonance imaging. *J Vasc Interv Radiol* 2010; 21:1347–1353

11. Goodwin SC, Spies JB. Uterine fibroid embolization. *N Engl J Med* 2009; 361:690–697

12. Pelage JP, Cazejust J, Pluot E, et al. Uterine fibroid vascularization and clinical relevance to uterine fibroid embolization. *RadioGraphics* 2005; 25(suppl 1):S99–S117

13. Isonishi S, Coleman RL, Hirama M, et al. Analysis of prognostic factors for patients with leiomyoma treated with uterine arterial embolization. *Am J Obstet Gynecol* 2008; 198:270.e1–270.e6

14. Kroencke TJ, Scheurig C, Poellinger A, Gronewold M, Hamm B. Uterine artery embolization for leiomyomas: percentage of infarction predicts clinical outcome. *Radiology* 2010; 255:834–841

15. Pelage JP, Guaou NG, Jha RC, Ascher SM, Spies JB. Uterine fibroid tumors: long-term MR imaging outcome after embolization. *Radiology* 2004; 230:803–809

16. Hagspiel KD, Matsumoto AH, Berr SS. Uterine fibroid embolization: assessment of treatment response using perfusion-weighted extraslice spin tagging (EST) magnetic resonance imaging. *J Magn Reson Imaging* 2001; 13:982–986

17. Li W, Brophy DP, Chen Q, Edelman RR, Prasad PV. Semiquantitative assessment of uterine perfusion using first pass dynamic contrast-enhanced MR imaging for patients treated with uterine fibroid embolization. *J Magn Reson Imaging* 2000; 12:1004–1008

18. Kim YS, Kim BG, Rhim H, et al. Uterine fibroids: semiquantitative perfusion MR imaging parameters associated with the intraprocedural and immediate postprocedural treatment efficiencies of MR imaging-guided high-intensity focused ultrasound ablation. *Radiology* 2014; 273:462–471

19. Liu J, Keserci B, Yang X, et al. Volume transfer constant (K(trans)) maps from dynamic contrast enhanced MRI as potential guidance for MR-guided high intensity focused ultrasound treatment of hypervascular uterine fibroids. *Magn Reson Imaging* 2014; 32:1156–1161

20. Kiguchi K, Kido A, Fujimoto K, et al. Non-contrast-enhanced MR angiography of uterine arteries with balanced steady-state free precession and time-space labelling inversion pulse: technical optimization and preliminary results. *Clin Radiol* 2014; 69:669–673

21. Lee MS, Kim MD, Lee M, et al. Contrast-enhanced MR angiography of uterine arteries for the prediction of ovarian artery embolization in 349 patients. *J Vasc Interv Radiol* 2012; 23:1174–1179

22. Mori K, Saida T, Shibuya Y, et al. Assessment of uterine and ovarian arteries before uterine artery embolization: advantages conferred by unenhanced MR angiography. *Radiology* 2010; 255:467–475

23. Mori K, Shiigai M, Ueda T, Kita N, Tanaka N, Minami M. Assessment of the uterine artery before uterine arterial embolization: comparison of unenhanced 3D water-excitation sensitivity-encoding time-of-flight (WEST) and gadolinium-enhanced 3D sensitivity-encoding water-excitation multishot echo-planar (SWEEP) MR angiography. *J Magn Reson Imaging* 2008; 27:557–562

24. Kroencke TJ, Scheurig C, Kluner C, Taupitz M, Schnorr J, Hamm B. Uterine fibroids: contrast-enhanced MR angiography to predict ovarian artery supply—initial experience. *Radiology* 2006; 241:181–189

25. Chen CL, Xu YJ, Liu P, et al. Characteristics of vascular supply to uterine leiomyoma: an analysis of digital subtraction angiography imaging in 518 cases. *Eur Radiol* 2013; 23:774–779

26. Frydrychowicz A, Wieben O, Niespodzany E, Reeder SB, Johnson KM, Francois CJ. Quantification of thoracic blood flow using volumetric magnetic resonance imaging with radial velocity encoding: in vivo validation. *Invest Radiol* 2013; 48:819–825

27. Stankovic Z, Allen BD, Garcia J, Jarvis KB, Markl M. 4D flow imaging with MRI. *Cardiovasc Diagn Ther* 2014; 4:173–192

28. Vasanawala SS, Hanneman K, Alley MT, Hsiao A. Congenital heart disease assessment with 4D flow MRI. *J Magn Reson Imaging* 2015; 42:870–886

29. Dyvorne H, Knight-Greenfield A, Jajamovich G, et al. Abdominal 4D flow MR imaging in a breath hold: combination of spiral sampling and dynamic compressed sensing for highly accelerated acquisition. *Radiology* 2015; 275:245–254

30. Stankovic Z, Rossle M, Euringer W, et al. Effect of TIPS placement on portal and splanchnic arterial blood flow in 4-dimensional flow MRI. *Eur Radiol* 2015; 25:2634–2640

31. Hsiao A, Lustig M, Alley MT, Murphy MJ, Vasanawala SS. Evaluation of valvular insufficiency and shunts with parallel-imaging compressed-sensing 4D phase-contrast MR imaging with stereoscopic 3D velocity-fusion volume-rendered visualization. *Radiology* 2012; 265:87–95

32. Saranathan M, Rettmann DW, Hargreaves BA, Clarke SE, Vasanawala SS. Differential subsampling with cartesian ordering (DISCO): a high spatio-temporal resolution Dixon imaging sequence for multiphasic contrast enhanced abdominal imaging. *J Magn Reson Imaging* 2012; 35:1484–1492

33. Cheng JY, Hanneman K, Zhang T, et al. Comprehensive motion-compensated highly accelerated 4D flow MRI with ferumoxytol enhancement for pediatric congenital heart disease. *J Magn Reson Imaging* 2016; 43:1355–1368

34. Stall L, Lee J, McCullough M, Nsrouli-Maktabi H, Spies JB. Effectiveness of elective unilateral uterine artery embolization: a case-control study. *J Vasc Interv Radiol* 2011; 22:716–722

35. Pelage JP, Le Dref O, Soyer P, et al. Arterial anatomy of the female genital tract: variations and relevance to transcatheter embolization of the uterus. *AJR* 1999; 172:989–994

36. Barth MM, Spies JB. Ovarian artery embolization supplementing uterine embolization for leiomyomata. *J Vasc Interv Radiol* 2003; 14:1177–1182

37. Rengier F, Delles M, Eichhorn J, et al. Noninvasive 4D pressure difference mapping derived from 4D flow MRI in patients with repaired aortic coarctation: comparison with young healthy volunteers. *Int J Cardiovasc Imaging* 2015; 31:823–830

38. Goubergrits L, Riesenkampff E, Yevtushenko P, et al. MRI-based computational fluid dynamics for diagnosis and treatment prediction: clinical validation study in patients with coarctation of aorta. *J Magn Reson Imaging* 2015; 41:909–916

39. Calkoen EE, Westenberg JJ, Kroft LJ, et al. Characterization and quantification of dynamic eccentric regurgitation of the left atrioventricular valve after atrioventricular septal defect correction with 4D flow cardiovascular magnetic resonance and retrospective valve tracking. *J Cardiovasc Magn Reson* 2015; 17:18

40. Meckel S, Leitner L, Bonati LH, et al. Intracranial artery velocity measurement using 4D PC MRI at 3 T: comparison with transcranial ultrasound techniques and 2D PC MRI. *Neuroradiology* 2013; 55:389–398
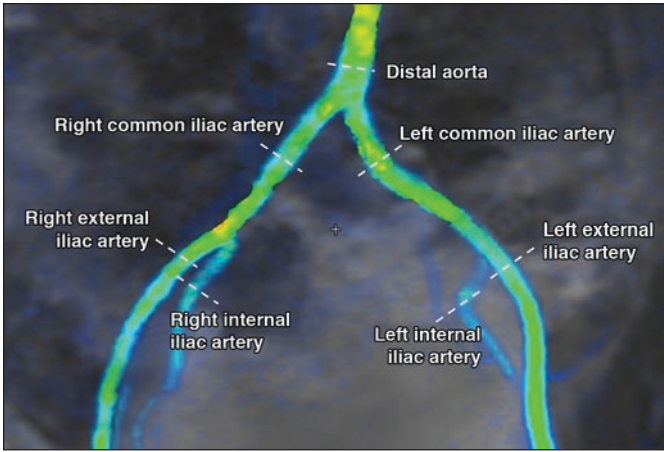
(Figures start on next page)

Fig. 1—Representative 4D flow MR image of 46-year-old female control subject with menorrhagia shows where flow measurements were obtained. All flow measurements were performed in triplicate at different locations along each vessel. No uterine fibroids were found.
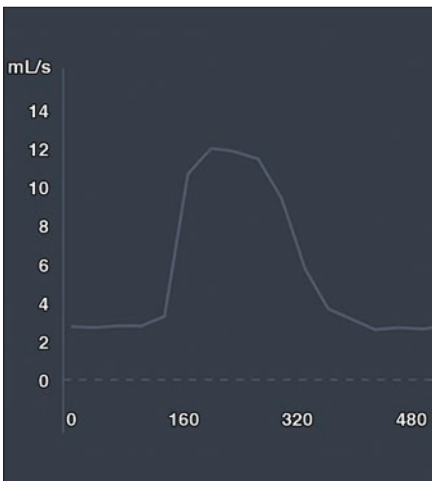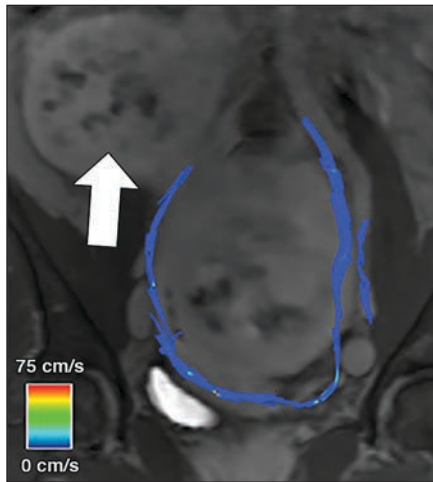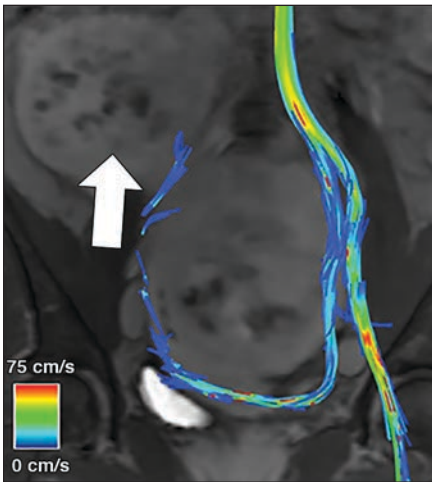

Fig. 2—55-year-old woman with large dominant midline fibroid and additional large pedunculated fibroid.

A and **B,** Streamline rendered vendor 4D flow images taken during systole (**A**) and diastole (**B**) show robust flow in left internal iliac and uterine arteries. Flow within left internal iliac artery was almost twice that of ipsilateral external iliac artery (0.31 vs 0.16 L/min, respectively). Large dominant midline fibroid and additional large pedunculated fibroid arising from right (*arrow*) are seen.

C, Graph of flow in milliliters per second (*y*-axis) plotted versus time in seconds (*x*-axis) throughout cardiac cycle obtained using Arterys CV Flow (Arterys) confirms robust flow in left internal iliac and uterine arteries.

D, Selective digital angiogram of left uterine artery confirms extensive supply to not only midline fibroid but also right pedunculated fibroid (*arrow*); these findings correlate to findings seen on 4D flow images (**A** and **B**). For uterine fibroid embolization, total of 5.5 mL of polyvinyl alcohol (PVA) embolic (0.5 mL of 200-μm PVA particles and 5.0 mL of 300-μm PVA particles) was needed to achieve stasis in left uterine artery, and 2.0 mL of PVA embolic (1.5 mL of 200-μm PVA particles and 0.5 mL of 300-μm PVA particles) was needed to achieve stasis in right uterine artery.
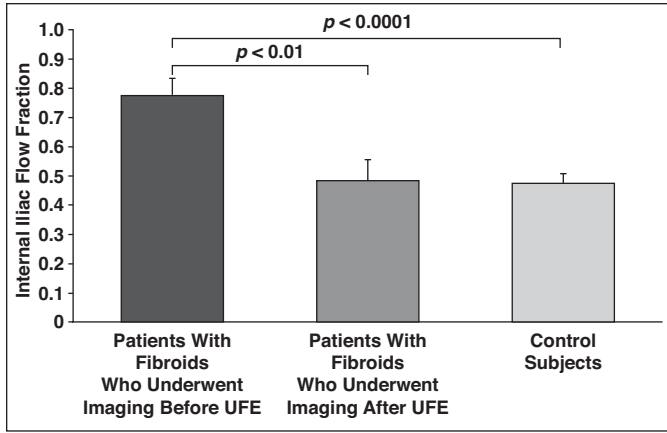
Fig. 3—Bar graph shows that 26 patients with fibroids who underwent 4D flow imaging before uterine fibroid embolization (UFE) had markedly elevated internal iliac flow fractions (mean ± standard error [SE], 0.78 ± 0.06) compared with seven patients with fibroids who underwent 4D flow imaging after UFE (0.48 ± 0.07, $p <$ 0.01) and seven control subjects (0.48 ± 0.08, $p < 0.0001$). Whiskers show mean ± 1 SE.
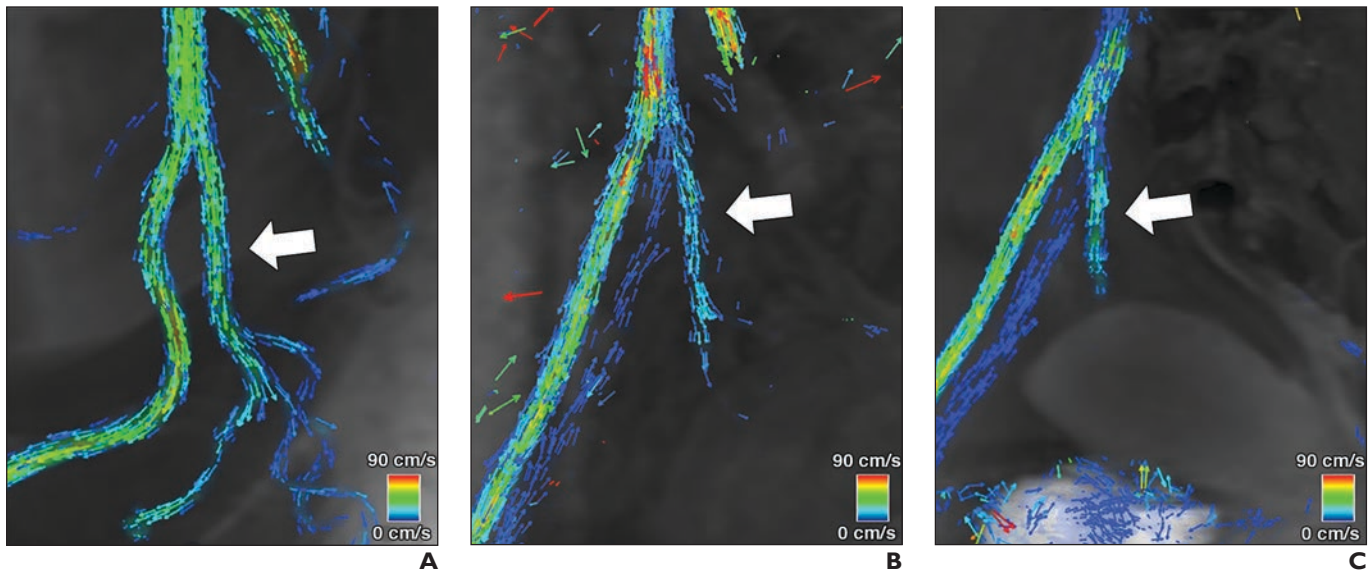

Fig. 4—Representative oblique vector overlay 4D flow views profiling external and internal iliac arteries side-by-side in patients with fibroids and control subject.
A–C, More robust flow in internal iliac artery (*arrows*) is clearly seen in 55-year-old woman with fibroids who underwent imaging before uterine fibroid embolization (UFE) (**A**) than in 30-year-old woman with fibroids who underwent imaging after UFE (**B**) and 37-year-old female control subject (**C**).
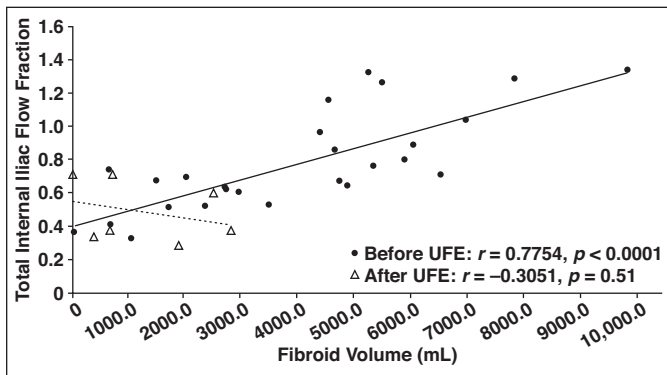
Fig. 5—Plot of fibroid volume versus total internal iliac flow fractions in patients with fibroids who underwent imaging before uterine fibroid embolization (UFE) (*circles*) and in patients with fibroids who underwent imaging after UFE (*triangles*). Internal iliac flow fractions correlated well with fibroid volumes before UFE ($r = 0.7754$, $p < 0.0001$) but not after UFE ($r = -0.3051$, $p = 0.51$). Solid line = linear regression of patients before UFE. Dotted line = linear regression of patients after UFE.
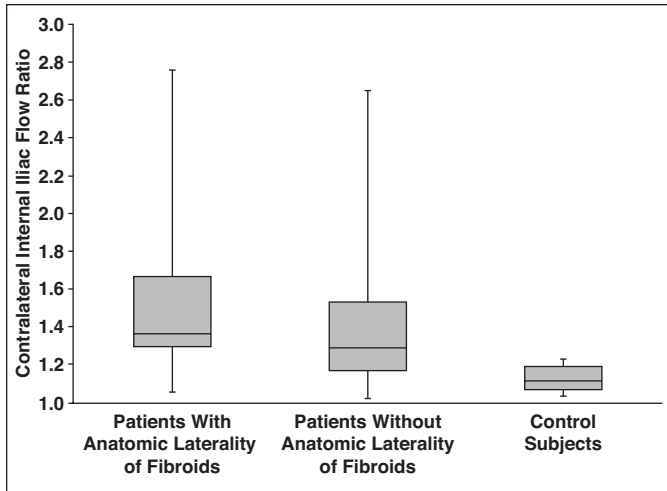
Fig. 6—Box-and-whisker plot shows quartile distribution of contralateral iliac flow ratios in fibroid patients with (excluding patients where flow and anatomic laterality did not match) and without anatomic laterality of their fibroids and in control subjects. Wide distribution of contralateral internal iliac flow ratios were seen in fibroid patients irrespective of whether they had anatomic laterality. In control subjects without fibroids, contralateral iliac flow ratios were lower and showed less variability than in patients with fibroids. Lines inside boxes = median, upper lines of boxes = third quartile, lower lines of boxes = first quartile, whiskers = maximum and minimum.
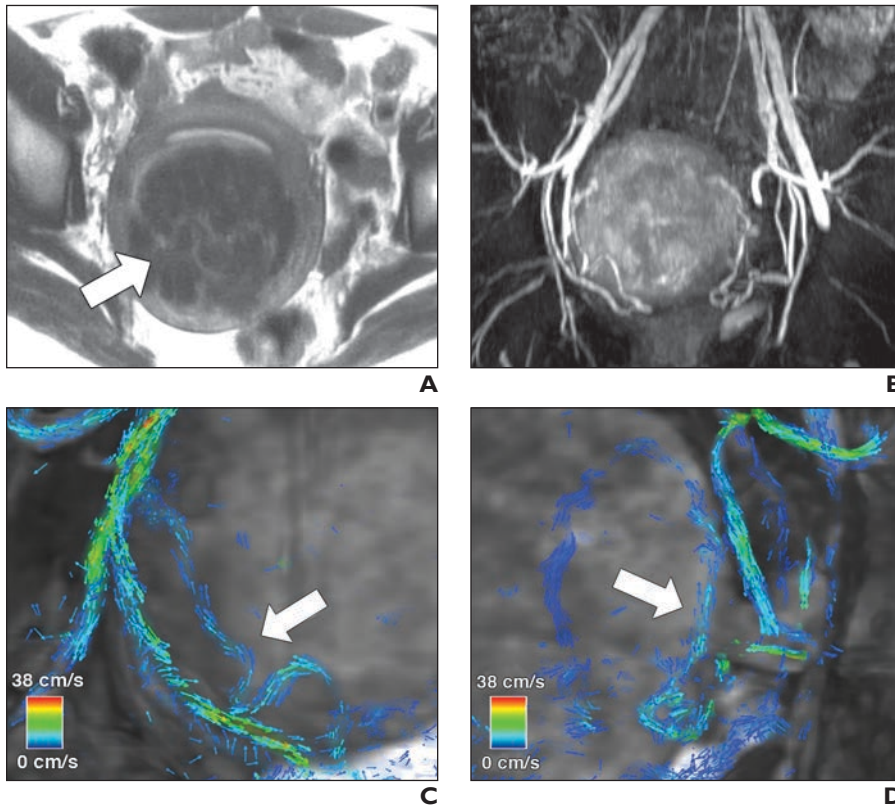
Fig. 7—Four-dimensional flow imaging may highlight differences in flow that are not apparent on conventional MR angiography or catheter angiography. In this example, patient is 34-year-old woman with single midline fibroid (patient 7 in Table 2). **A** and **B,** T2-weighted image (**A**) and MR angiogram (**B**) show single midline fibroid with apparent equal contribution from both uterine arteries (*arrow*, **A**). **C** and **D,** Four-dimensional flow images obtained before uterine fibroid embolization (UFE) of right side (**C**) and left side (**D**) show higher flow in right internal iliac artery than in left internal iliac artery (*arrows*) (0.26 vs 0.17 L/min, respectively).

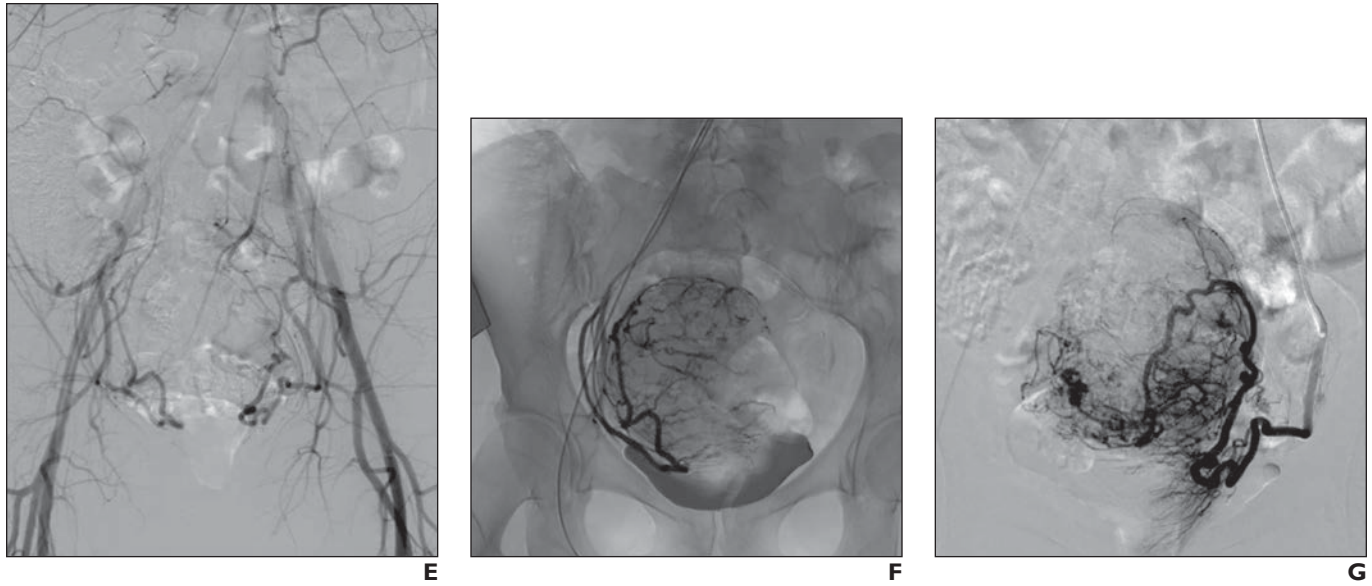**(Fig. 7 continues on next page)**

Fig. 7 (continued)—Four-dimensional flow imaging may highlight differences in flow that are not apparent on conventional MR angiography or catheter angiography. In this example, patient is 34-year-old woman with single midline fibroid (patient 7 in Table 2).

E, Pelvic aortogram (iodixanol [Visipaque 320, GE Healthcare] administered at 15 mL/s for 2 seconds) obtained at subsequent UFE shows roughly equal conspicuity of both uterine arteries with each supplying large proportion of fibroid on subsequent selective injections.

F and **G,** Right uterine digital angiogram (**F**) and left uterine digital subtraction angiogram (**G**). Right side required more than twice as much volume of embolic to achieve stasis (0.5 mL of 200-μm polyvinyl alcohol [PVA] particles and 3.0 mL of 300-μm PVA particles) compared with left (0.5 mL of 200-μm PVA particles and 1.0 mL of 300-μm PVA particles).
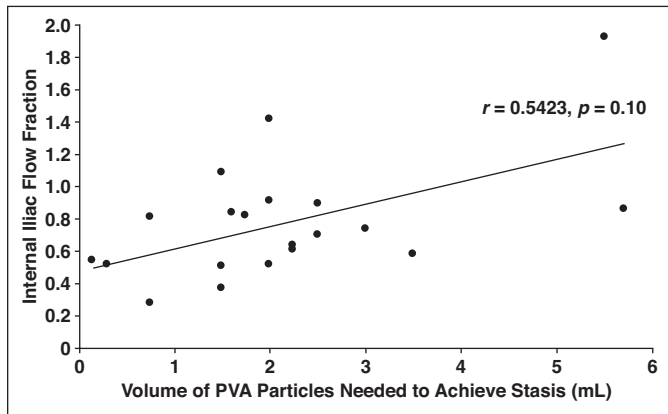

Fig. 8—Internal iliac flow as measured by 4D flow correlates with volume of embolic required to achieve stasis.

A, Graph shows positive correlation between volume of polyvinyl alcohol (PVA) embolic required to achieve stasis on each side and unilateral internal iliac flow fractions ($r = 0.5423$, $p = 0.10$). Solid line = linear regression.

B, Graph shows positive correlation between volume of PVA embolic required to achieve stasis on each side and gross internal iliac artery flow ($r = 0.4156$, $p = 0.23$). Solid line = linear regression.

C, Graph shows stronger positive correlation between ratio of PVA embolic required to achieve stasis between sides and contralateral internal iliac flow ratio ($r = 0.6776$, $p = 0.03$). Solid line = linear regression.
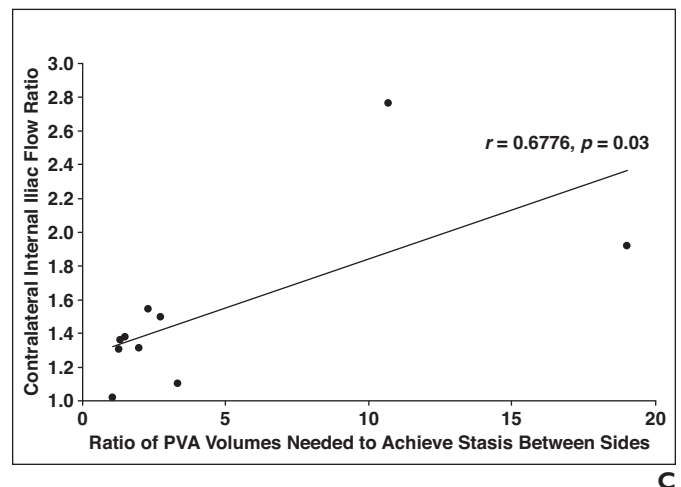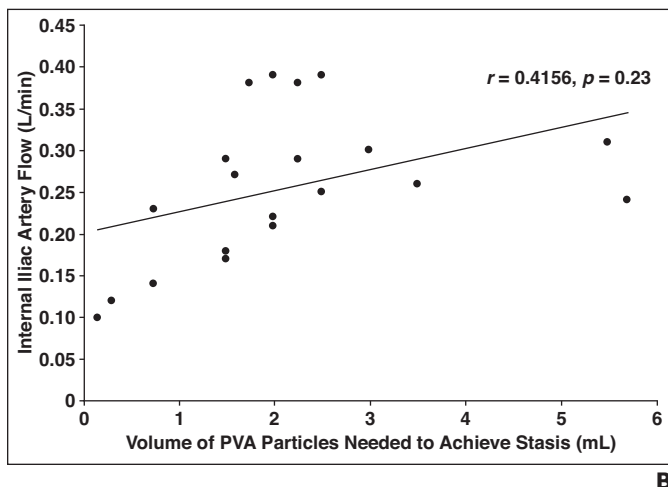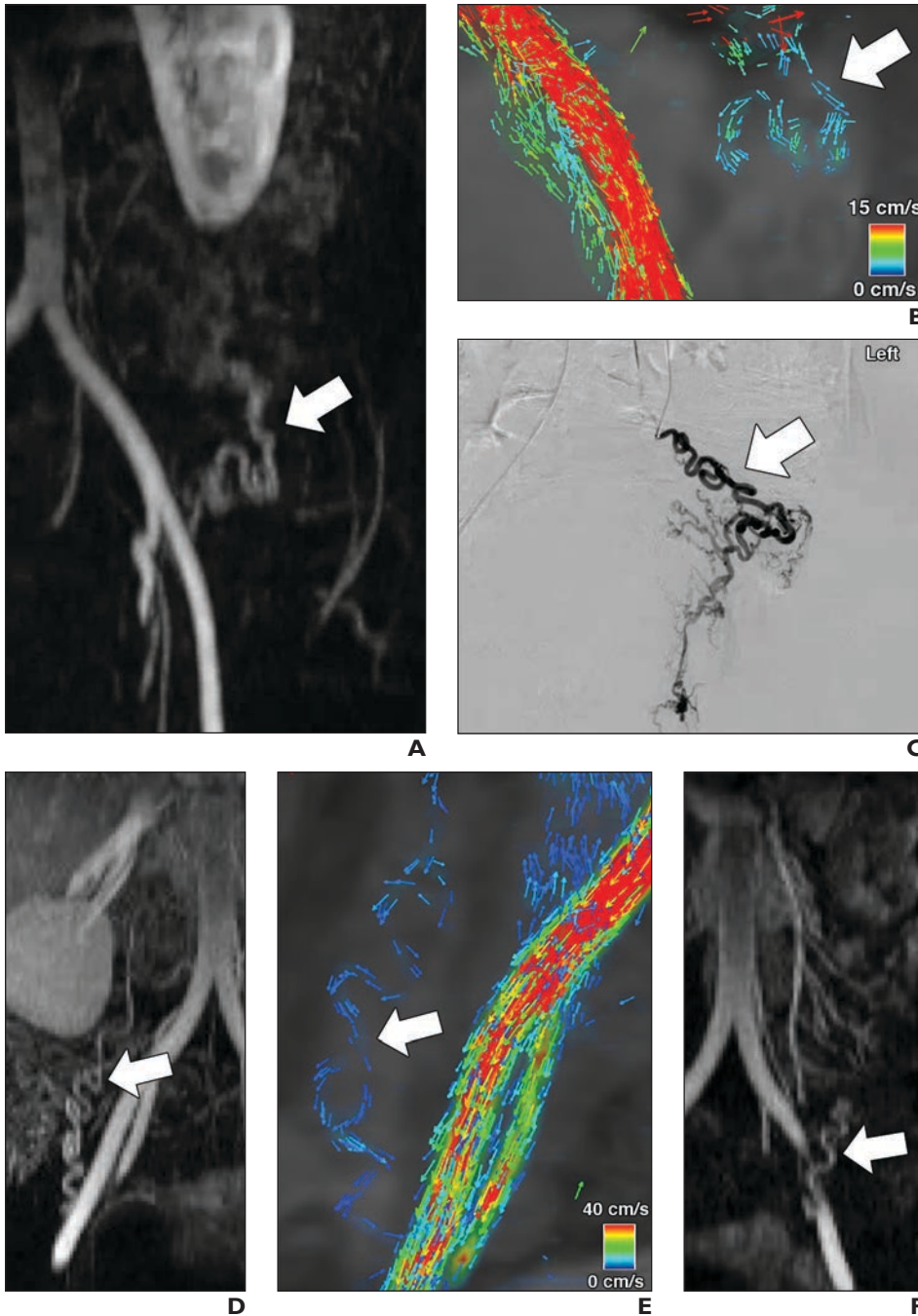
Fig. 9—Four-dimensional flow imaging can measure contribution of ovarian artery to flow to uterine fibroids.
A–C, MR angiogram (**A**), 4D flow image (**B**), and left ovarian angiogram (**C**) of 41-year-old woman with fibroids. MR angiogram shows left ovarian artery supply (*arrow*, **A**) to left side of single right-sided fibroid. Four-dimensional image shows flow of left ovarian artery (*arrow*, **B**) is 0.04 L/min. Subsequent left ovarian angiogram obtained at uterine fibroid embolization confirms that ovarian artery (*arrow*, **C**) is supplying fibroids. Fibroids were then embolized with 0.75 mL of 200-μm polyvinyl alcohol particles.
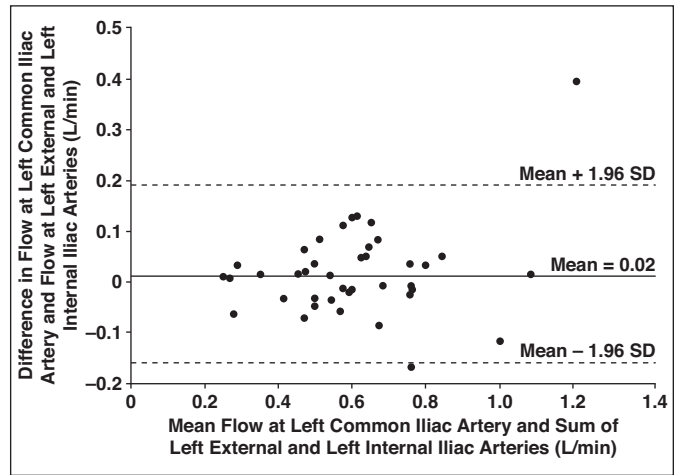**D–G,** MR angiogram (**D**) and 4D flow image of right ovarian artery (**E**) and MR angiogram (**F**) and 4D flow image of left ovarian artery (**G**) of 45-year-old woman with fibroids. Images show bilateral ovarian artery supply to fibroids (*arrows*). Right ovarian artery flow was measured at 0.03 L/min, and left ovarian artery flow was measured at 0.04 L/min.
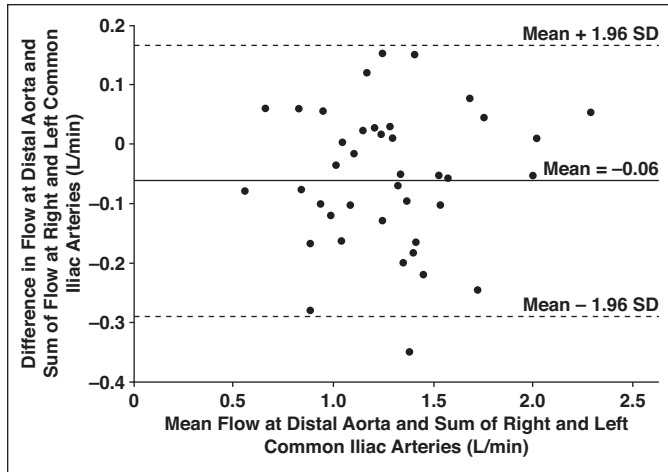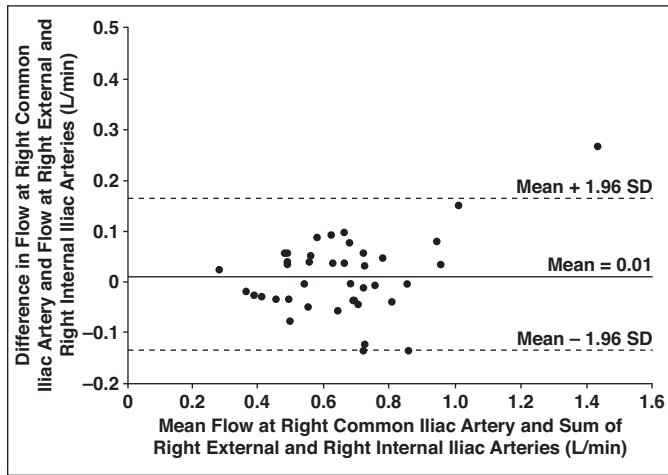
Fig. 10—Consistency of 4D flow measurements were confirmed with Bland-Altman plots.
A, Flow at distal abdominal aorta was compared with sum of flows of bilateral common iliac arteries.
B and **C,** Flow of right (**B**) and left (**C**) common iliac arteries were compared with sum of their respective downstream external and internal iliac arteries. Almost all measurements fell within 2 SDs of flow differences between vessel of interest and its downstream counterparts, indicating internal consistency of measurements.